Langmuir-Hinshelwood-Hougen-Watson Heterogeneous Kinetics Model for the Description of Fe (II) Ion Exchange on Na-X Zeolite

Sanarya K. Kamal
Chemical Engineering Department
College of Engineering
University of Baghdad
Baghdad, Iraq
sanarya.kamal1507d@coeng.uobaghdad.edu.iq

Ammar S. Abbas
Chemical Engineering Department
College of Engineering
University of Baghdad
Baghdad, Iraq
ammarabbas@coeng.uobaghdad.edu.iq

Abstract-This study aimed to investigate the kinetics of the anion exchange step of ferrous ions with Na-X zeolite in a temperature range of 20 and 80°C for a period of up to 8 hours. A ferrous sulfate heptahydrate solution was used as a ferrous ion source to exchange with the sodium of the Na-X zeolite. The results showed a change in the physical appearance of the zeolite with the progress of the ion exchange process. The catalyst color was observed with the progress of the ion exchange time and changed from yellow to brown. The ferrous ion exchanged contents increased with temperature and reached 0.519 at 80°C after 8 hours. A kinetic model based on the Langmuir-Hinshelwood-Hougen-Watson model was suggested and developed to describe the ion-exchange process. The proposed model was solved numerically, and the results indicated its ability to describe the experimental results with high correlation coefficients. Finally, the activation energy for the forward reaction was 31590.7J/mole compared to 28105.5J/mole for the backward, and the frequency factors for the forward and backward reactions were investigated.

Keywords-Fe exchanged; Na-X zeolite; ion exchange; anion capacity

I. INTRODUCTION

Zeolites are microporous, crystalline aluminosilicates with a unique mix of physical and chemical properties that make them excellent for a wide range of uses in industry [1-3], agriculture, medicine [4], and environmental pollution cleanup [5]. Na-X zeolites are synthetic zeolites that have been used and investigated in industrial chemicals as ion exchangers, sorbents [5, 6], and catalysts [7] due to their significant void volume of 50% of the frame structure, their ion exchange capacity, shape selectivity, and solid acid sites [8, 9]. The structure of Na-X zeolites is a Faujasite framework with a cage made up $Na_{86}[(AlO_2)_{86}(SiO_2)_{106}].H_2O$ with a ratio of 1-1.5 joined together by bridging oxygen atoms resulting in a 12-ring pore opening and 3-dimensional channel system [10].

The negative charges of AlO_4 units are balanced by sodium cations (Na^+) which are exchanged by other cations such as CO^{2+}, Cu^{2+}, Zn^{+2}, and Cr^{+3} ions in the solution [11, 12]. Because of the destruction of the zeolite framework, the exchange capacity of Na-X zeolites makes them particularly effective adsorbents or catalysts. Metal-containing zeolites are especially appealing [13]. Iron-containing zeolites can be used as heterogeneous Fenton or photo-Fenton catalysts [14] and utilized to remove organic pollutants in water treatment plants [15, 16]. Transition metal-containing zeolites are manufactured using a variety of methods including: (i) ion exchange from aqueous solution [11, 17, 18] or solid-state reaction [19], (ii) hydrothermal synthesis [20], and (iii) adsorption and decomposition of volatile organometallic compounds [21, 22]. Ion exchange from an aqueous solution is frequently used to introduce transition metal ions into Na-X zeolites. The mechanics and outcomes are not always straightforward. Transition metal ions may usually replace only a portion of the original cations, which are mainly sodium ions [23].

Ferrous ions (Fe (II)), which are frequently introduced into Na-X zeolites by ion exchange, can coordinate with oxygen atoms more selectively than filling the shell cations and have easy access to other oxidation states [24], so their introduction into zeolites leads to new mechanisms for their function as sorbents [14] and catalysts [25]. However, because ion exchange is reversible, once adsorbed nuclides in water are exchanged by other cations (Na^+, Ca^{2+}, Mg^{2+}, etc.) [26]. This research aimed to study the effect of temperature and time on the Fe (II) exchange process with Na on the X zeolite. A heterogeneous kinetics model was developed to describe the exchange process based on the heterogeneous Langmuir-Hinshelwood-Hougen-Watson (LHHW) approach.

II. EXPERIMENTAL PROCESS

The zeolite used was the type Na-X zeolite (commercial grain, Si/Al ratio 1.75, pore volume 0.2733cm³/g, surface area 450m²/g, initial Na=14.719%), which was crushed and then sieved with 200 mesh strainers to homogenize its size. 40g of zeolite were weighed and then washed with distilled water. Afterward, they were washed with deionized water at various

---

Corresponding author: Ammar S. Abbas

times, the Na-X zeolite was filtered by filter paper (Chm F1002 filter paper,150mm, penetration range (7-8μm)), went through a Buckner funnel, a vacuum pump, and then was dried at 60°C overnight in an oven (Memmert, Sigma, England UK). Na-X was mashed by crushing until powder again. The activation process was carried out using a 0.1N chloride acid solution (36.5% HCl, USA) to clean the pore surface of zeolite and remove impurities. The cleaning HCl acid solution was mixed with Na-X zeolite in a 10:1 ratio (v/w ratio) and stirred with a hot plate magnetic stirrer (Thermo Fisher Scientific Inc, USA) for 1 hour at 250rpm at 25°C [27]. The HCl solution was separated from the Na-X zeolite using filter paper, washed with distilled water, and stopped until a neutral pH=7 was obtained. The activated Na-X zeolite was dried at 60°C overnight. The calcination of the cleaning Na-X zeolite samples was obtained at 550°C for 3 hours with a furnace (Carbonite, Sigma, England UK). After cooling, the samples were stored in a desiccator to prevent water absorption. Then, Na-X zeolite containing a high sodium weight percentage (14.719%) was exposed to an ion exchange procedure with ferrous sulfate heptahydrate ($FeSO_4·7H_2O$, India) to replace the sodium from Na-X zeolite. This procedure was carried out in beakers with a volume of 0.5lt, under controlled temperatures (20, 40, 60, and 80°C) and were stirred again. 5g of dried Na-X zeolite were added to 100ml of a 0.319M solution and maintained at the required temperature with constant stirring at 300rpm for 8 hours. Subsequently, exchanged Na-X zeolite samples were taken from the ion-exchanged solution and filtered, washed several times with distilled water to remove the Fe (II) that was not exchanged, and taken to an oven to dry at 60°C overnight. The samples were calcined in a furnace at 550°C for 3 hours, and were left to cool inside desiccator until they reached room temperature. The concentration of Fe (II) in the exchange solution was measured using atomic absorption spectrophotometry (VarianAA240FS, Australia), and the amount of exchange Fe (II) was determined. The atomic absorption spectrophotometry was tested at North Gas Company (Ministry of Oil, Iraq).

III. RESULTS AND DISCUSSION

The ion exchange reaction was carried out between Na-X zeolite and ferrous sulfate solution with a stoichiometric amount of Fe/Na at different temperatures for a processing time up to 8 hours. At first, the color of the catalyst was observed with the progression of the ion exchange process. A darker yellowish-brown product was generally obtained with increasing ion-exchange time and processing temperature. Figure 1 depicts three zeolites: original Na-X zeolite, activated Na-X zeolite, and X zeolite after Fe (II) ions were exchanged for 8 hours at 80°C. The color change of the treated zeolite indicated that Fe-13X was formed.
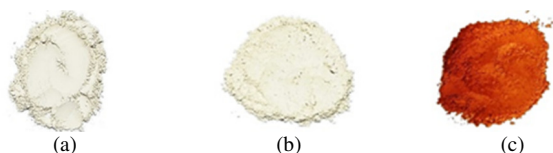

Fig. 1.   Color of (a) Na-X Zeolite, (b) Na-X activated, and (c) Modified Fe-13X for 8 hours at 80°C.

The amount of Fe (II) conversion versus time and temperature by ion exchange reaction is shown in Figure 2. Figure 2 shows that the Fe (II) ion exchange (conversion) increased with the reaction time and temperature, and the results showed a rapid increase during the first 0.25h, after which the conversion increased slowly and reached a similar to the equilibrium state at the end of the studied time. The conversion accelerated with the reaction time as the temperature increased. The conversion was 0.179 after 0.25h of reaction at 20°C, whereas it was 0.415 after the same period at 80°C, while the higher required value of Fe (II) conversion was 0.519 obtained after 8h of ion exchange at 80°C. These results agree with the Cobalt exchange on Na-X zeolite previously found in [28].
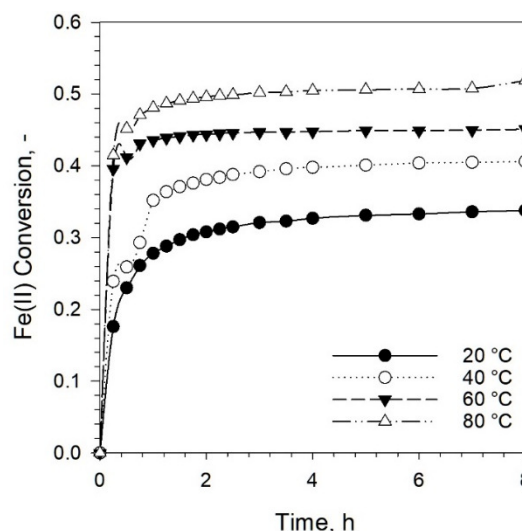

Fig. 2.   Fe (II) conversion on the Na-X zeolite versus time at different temperatures.

Langmuir-Hinshelwood-Hougen-Watson (LHHW) kinetics model assumes that before the surface reaction, the Fe (II) is adsorbed onto the catalyst surface. The final stage of the mechanism involves the desorption of Na ions. The surface reaction (1) was assumed to be the rate-controlling step, and the LHHW kinetics model performing the ion exchange can be written as (2) - (11).

$$Fe^{+2}{}_{(aq)} + Na - X_{(surface)} \overset{k_s k_s'}{\rightleftarrows} zNa^+{}_{(aq)} + Fe - X_{(surface)} \quad (1)$$
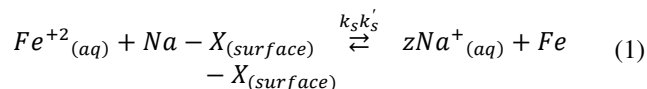
$$-r_{Fe^{+2}{}_S} = k_s\left(C_{Fe^{+2}{}_S}C_{Na-X_S} - \frac{1}{K_S}C_{zNa^+{}_S}C_{Fe-X_S}\right) \quad (2)$$

The adsorbed phase concentrations can be written as:

$$C_{Fe^{+2}{}_S} = K_{Fe^{+2}}C_{Fe^{+2}}C_v \quad (3)$$

$$C_{zNa^+{}_S} = K_{zNa^+}C_{zNa^+}C_v \quad (4)$$

Substituting these values in (3) and (4) into (2) gives:

$$-r_{Fe^{+2}S} = k_s \left(K_{Fe^{+2}} C_{Fe^{+2}} C_v K_{Na-X} C_{Na-X} C_v - \frac{1}{K_s} K_{zNa^+} C_{zNa^+} C_v K_{Fe-X} C_{Fe-X} C_v \right) \quad (5)$$

Now,

$$C_{Fe^{+2}_o} = C_{Fe^{+2}_s} + C_{zNa^+_s} + C_v \quad (6)$$

which can be simplified into:

$$C_{Fe^{+2}_o} = C_v (K_{Fe^{+2}} C_{Fe^{+2}} + K_{zNa^+} C_{zNa^+} + 1) \quad (7)$$

Finally, solving for C_v gives:

$$C_v = \frac{C_{Fe^{+2}_o}}{(K_{Fe^{+2}} C_{Fe^{+2}} + K_{zNa^+} C_{zNa^+} + 1)} \quad (8)$$

By substituting and simplifying, this can be rewritten as:

$$-r_{Fe^{+2}S} = k_S K_{Fe^{+2}} K_{zNa^+} (C_{Fe^{+2}})_o \left(\frac{\frac{C_{Fe^{+2}} C_{Na-X}}{K_{zNa^+}} - \frac{C_{zNa^+} C_{Fe-X}}{K_S K_{Fe^{+2}}}}{1 + K_{Fe^{+2}} C_{Fe^{+2}} + K_{zNa^+} C_{zNa^+}} \right) \quad (9)$$

$$K_S = \frac{C_{zNa^+_s}}{C_{Fe^{+2}_s}} = \frac{k_s}{k_s'} \quad (10)$$

$$K = \frac{K_{Fe^{+2}}}{K_{zNa^+}} \cdot K_S \quad (11)$$

where C_{Fe+2} is the concentration of Fe (II) in the solution, C_{Na-X} is the concentration of the catalyst Na-X zeolite, C_{zNa+} is the concentration of Na^+ in the solution, C_{Fe-X} is the concentration of Fe exchanged on the zeolite, k_s is the forward surface reaction rate constant, $k_{s'}$ is the backward surface reaction constant, K_s is the equilibrium constant for exchange surface reaction, and K_{Fe} and K_{Na} are the equilibrium constants for Fe (II), and Na^+ respectively. The correlation coefficient (R^2) is presented in (12):

$$R^2 = \frac{(\Sigma_{i=1}^n (r_{Fe^{+2}exp} - \overline{r_{Fe^{+2}exp}})(r_{Fe^{+2}cal} - \overline{r_{Fe^{+2}cal}}))^2}{\Sigma_{i=1}^n (r_{Fe^{+2}exp} - \overline{r_{Fe^{+2}exp}})^2 \times \Sigma_{i=1}^n (r_{Fe^{+2}cal} - \overline{r_{Fe^{+2}cal}})^2} \quad (12)$$

where $r_{Fe}{}^{+2}_{exp}$ is the experimental reaction rate, $r_{Fe}{}^{+2}_{cal}$ is the calculated reaction rate from the model, and ($^-$) represents average value. The kinetics equation was solved numerically using the damped least-squares method with the Levenberg-Marquardt algorithm by finding the reaction rate constant and

the values of the equilibrium constants at each temperature, which gives a reaction rate approximating the experimental reaction speed, which was obtained by maximizing the R^2 value (12) at each temperature. Figure 3 shows the relationship between the reaction rate values calculated from the model and the experimental values. Figure 3 also shows that the model rate values were slightly higher than the experimental rates at low reaction rate values, but in general, the model excellently described the experimental results with a high R^2.
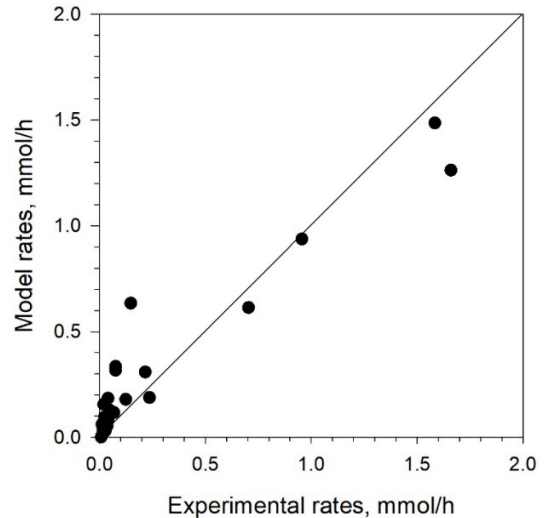

Fig. 3.   Relation between the experimental and model rates.

The results of the model solution, including the values of the reaction rate and the equilibrium constants, and the values of R^2 for each temperature, are summarized in Table I. As can be noted, the values of k_s, $k_{s'}$, and K_s increased with the temperature of the ion exchange process. The increase in the values of k_s, $k_{s'}$, and K_s with increasing temperature and the values of k_s remaining higher than the values of $k_{s'}$ indicated that the reaction of ion exchange of Fe (II) with sodium improved with increasing temperature. The results of the model solution also showed that the values of K_{Fe} and K_{Na} lowered with the increase in temperature, indicating that the quantities at the catalyst surface of these two substances decrease with temperature rise.

TABLE I.   REACTION RATE CONSTANT VS DIFFERENT TEMPERATURES

Temperature, °C	k_s, 1/liter.mmol.h	K_S	$k_{s'}$, 1/liter.mmol.h	K_{Fe}	K_{Na}
20	10.1997	1.1318	9.0119	59.9865	1.8494
40	63.5805	1.2086	52.607	21.3015	1.6658
60	84.7414	1.2661	66.931	5.4395	1.3750
80	100.6624	1.4658	68.674	4.3195	1.2513

Activation energies and frequency pre-exponential factors were calculated for both the forward and backward reaction constants (k_s, or $k_{s'}$) using the Arrhenius equation [29]. The linear form of the Arrhenius equation is:

$$ln(k_i) = ln(A) - \frac{E}{RT} \quad (13)$$

where k_i is the rate constant (k_s, or $k_{s'}$), T is the absolute temperature in Kelvin, A is the pre-exponential factor for the

chemical reaction, E is the reaction activation energy, and R is the general gas constant. Figure 4 shows the linear form of the Arrhenius equation, and the activation energy and frequency factor values were calculated for each of the forward and the back reactions of the ion exchange process.

The activation energies were 31590.7J/mole for the forward reaction and 28105.5J/mole for the backward. The value of the frequency factor for the forward reaction was higher than for

the backward (6596171.7 versus 1418343.2). The large value of the activation energy of the forward reaction relative to the backward supports the fact that the ion exchange process improves with increasing temperature, which was experimentally observed.
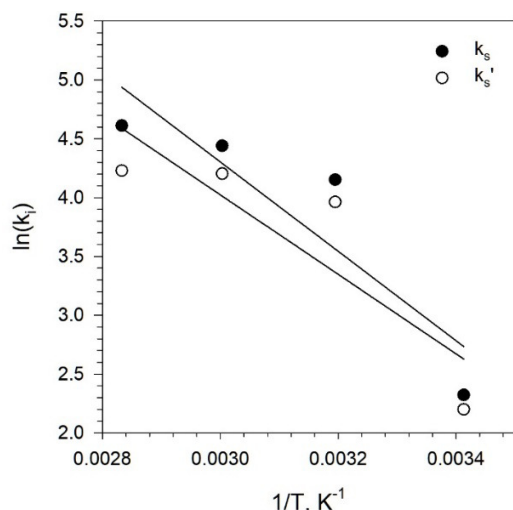

Fig. 4.   Arrhenius plot of Fe exchange kinetics.

IV.   CONCLUSION

The Fe (II) exchanged Na-X zeolite was prepared by the ion exchange method from a $FeSO_4.7H_2O$ solution. The catalyst color changed from yellow to dark brown with the ion exchange progress and increased temperature. The Fe (II) exchanged contents increased with temperature and reached 0.519 at 80°C after 8 hours. An LHHW heterogeneous kinetics model was developed and used to describe the ion-exchange experimental data. The results indicated the ability of the model to describe the experimental results with high correlation coefficients. In general, the values of the reaction constant and reaction equilibrium constant increased with temperature, while the equilibrium constants of the reactant and the products on the zeolite surface decreased. The activation energies were 31590.7J/mole and 28105.5J/mole for the forward and backward reactions, therefore, it can be concluded that higher temperature improves the ion exchange process.

REFERENCES

[1]   A. H. A. K. Mohammed and M. M. Abdul-Raheem, "Adsorption of BTX Aromatic from Reformate by 13X Molecular Sieve," *Iraqi Journal of Chemical and Petroleum Engineering*, vol. 9, no. 4, pp. 13–20, Dec. 2008.

[2]   A. H. A. K. Mohammed and M. K. Baki, "Separation Benzene and Toluene from BTX using Zeolite 13X," *Iraqi Journal of Chemical and Petroleum Engineering*, vol. 9, no. 3, pp. 21–25, Sep. 2008.

[3]   A. H. El-Sinawi, "Production of Hydrogen from Poly Ethylene Terephthalate (PET) using CT 434 ZSM-5 Catalyst at Considerably Low Temperatures," *Engineering, Technology & Applied Science Research*, vol. 6, no. 6, pp. 1269–1273, Dec. 2016, https://doi.org/10.48084/etasr.822.

[4]   A. Elfiad, D. C. Boffito, S. Khemassia, F. Galli, S. Chegrouche, and L. Meddour-Boukhobza, "Eco-friendly synthesis from industrial wastewater of Fe and Cu nanoparticles over NaX zeolite and activity in 4-nitrophenol reduction," *The Canadian Journal of Chemical Engineering*, vol. 96, no. 7, pp. 1566–1575, 2018, https://doi.org/10.1002/cjce.23083.

[5]   S. K. A. Barno, H. J. Mohamed, S. M. Saeed, M. J. Al-Ani, and A. S. Abbas, "Prepared 13X Zeolite as a Promising Adsorbent for the Removal of Brilliant Blue Dye from Wastewater," *Iraqi Journal of Chemical and Petroleum Engineering*, vol. 22, no. 2, pp. 1–6, Jun. 2021, https://doi.org/10.31699/IJCPE.2021.2.1.

[6]   R. T. Yang, *Adsorbents: Fundamentals and Applications*. Hoboken, NJ, USA: John Wiley & Sons, 2003.

[7]   "Comparative Study on the Catalytic Performance of a 13X Zeolite and its Dealuminated Derivative for Biodiesel Production," *Bulletin of Chemical Reaction Engineering & Catalysis*, vol. 16, no. 4, pp. 763–772, Aug. 2021, https://doi.org/10.9767/bcrec.16.4.11436.763-772.

[8]   K. Y. Foo and B. H. Hameed, "The environmental applications of activated carbon/zeolite composite materials," *Advances in Colloid and Interface Science*, vol. 162, no. 1, pp. 22–28, Feb. 2011, https://doi.org/10.1016/j.cis.2010.09.003.

[9]   A. Corma, "State of the art and future challenges of zeolites as catalysts," *Journal of Catalysis*, vol. 216, no. 1, pp. 298–312, May 2003, https://doi.org/10.1016/S0021-9517(02)00132-X.

[10]   B. A. Alshahidy and A. S. Abbas, "Preparation and modification of 13X zeolite as a heterogeneous catalyst for esterification of oleic acid," *AIP Conference Proceedings*, vol. 2213, no. 1, Mar. 2020, Art. no. 020167, https://doi.org/10.1063/5.0000171.

[11]   S. Bendenia, K. Marouf-Khelifa, I. Batonneau-Gener, Z. Derriche, and A. Khelifa, "Adsorptive properties of X zeolites modified by transition metal cation exchange," *Adsorption*, vol. 17, no. 2, pp. 361–370, Apr. 2011, https://doi.org/10.1007/s10450-011-9336-4.

[12]   J. R.Ugal, M. Mustafa, and A. A.Abdulhadi, "Preparation of Zeolite Type 13X from Locally Available Raw Materials," *Iraqi Journal of Chemical and Petroleum Engineering*, vol. 9, no. 1, pp. 51–56, Mar. 2008.

[13]   P. C. Silva, N. P. Ferraz, E. A. Perpetuo, and Y. J. O. Asencios, "Oil Produced Water Treatment Using Advanced Oxidative Processes: Heterogeneous-Photocatalysis and Photo-Fenton," *Journal of Sedimentary Environments*, vol. 4, no. 1, pp. 99–107, Mar. 2019, https://doi.org/10.12957/jse.2019.40991.

[14]   S. Navalon, M. Alvaro, and H. Garcia, "Heterogeneous Fenton catalysts based on clays, silicas and zeolites," *Applied Catalysis B: Environmental*, vol. 99, no. 1, pp. 1–26, Aug. 2010, https://doi.org/10.1016/j.apcatb.2010.07.006.

[15]   H. A. Maddah, "Numerical Analysis for the Oxidation of Phenol with TiO2 in Wastewater Photocatalytic Reactors," *Engineering, Technology & Applied Science Research*, vol. 8, no. 5, pp. 3463–3469, Oct. 2018, https://doi.org/10.48084/etasr.2304.

[16]   R. M. Galvin, "Evaluating Pollutants of Emerging Concern in Aquatic Media Through E-PRTR Regulation. A Case Study: Cordoba, Spain, 2009-2018," *Engineering, Technology & Applied Science Research*, vol. 9, no. 5, pp. 4795–4800, Oct. 2019, https://doi.org/10.48084/etasr.3130.

[17]   S. Bendenia, K. Marouf-Khelifa, I. Batonneau-Gener, Z. Derriche, and A. Khelifa, "Adsorptive properties of X zeolites modified by transition metal cation exchange," *Adsorption*, vol. 17, no. 2, pp. 361–370, Apr. 2011, https://doi.org/10.1007/s10450-011-9336-4.

[18]   N. Rajamohan, R. R. Kannan, and M. Rajasimman, "Kinetic Modeling and Effect of Process Parameters on Selenium Removal Using Strong Acid Resin," *Engineering, Technology & Applied Science Research*, vol. 6, no. 4, pp. 1045–1049, Aug. 2016, https://doi.org/10.48084/etasr.635.

[19]   R. M. Haniffa and K. Seff, "Partial structures of solid-state copper(II)-exchanged zeolite Y and its D2O sorption complex by pulsed-neutron diffraction," *Microporous and Mesoporous Materials*, vol. 25, no. 1, pp. 137–149, Dec. 1998, https://doi.org/10.1016/S1387-1811(98)00196-6.

[20]   P. Feng, X. Bu, and G. D. Stucky, "Hydrothermal syntheses and structural characterization of zeolite analogue compounds based on cobalt phosphate," *Nature*, vol. 388, no. 6644, pp. 735–741, Aug. 1997, https://doi.org/10.1038/41937.

[21]   J. G. Jee, M. K. Park, H. K. Yoo, K. Lee, and C. H. Lee, "Adsorption and Desorption Characteristics of Air on Zeolite 5a, 10x, and 13x Fixed

Beds," *Separation Science and Technology*, vol. 37, no. 15, pp. 3465–3490, Jan. 2002, https://doi.org/10.1081/SS-120014437.

[22] W. Shen and B. J. Shen, "Synthesis and Characterization of Composite Structure Zeolite Y," *Advanced Materials Research*, vol. 233–235, pp. 1790–1793, 2011, https://doi.org/10.4028/www.scientific.net/AMR.233-235.1790.

[23] F. Heinrich, C. Schmidt, E. Löffler, and W. Grünert, "A highly active intra-zeolite iron site for the selective catalytic reduction of NO by isobutane," *Catalysis Communications*, vol. 2, no. 10, pp. 317–321, Dec. 2001, https://doi.org/10.1016/S1566-7367(01)00056-5.

[24] S. Kumar and S. Jain, "History, Introduction, and Kinetics of Ion Exchange Materials," *Journal of Chemistry*, vol. 2013, Oct. 2013, Art. no. e957647, https://doi.org/10.1155/2013/957647.

[25] I. C. Ostroski, M. A. S. D. Barros, E. A. Silva, J. H. Dantas, P. A. Arroyo, and O. C. M. Lima, "A comparative study for the ion exchange of Fe(III) and Zn(II) on zeolite NaY," *Journal of Hazardous Materials*, vol. 161, no. 2, pp. 1404–1412, Jan. 2009, https://doi.org/10.1016/j.jhazmat.2008.04.111.

[26] M. N. Rashed and P. N. Palanisamy, "Introductory Chapter: Adsorption and Ion Exchange of Zeolites for Treatment of Polluted Water," in *Zeolites and Their Applications*, London, UK: InTechOpen, 2018.

[27] H. Nasution, H. Harahap, S. Pandia, D. M. Putra, and M. T. A. Fath, "Characterizations of activated zeolite using hydrolysis method," *AIP Conference Proceedings*, vol. 2175, no. 1, Nov. 2019, Art. no. 020019, https://doi.org/10.1063/1.5134583.

[28] H.-L. Tran, M.-S. Kuo, W.-D. Yang, and Y.-C. Huang, "Study on Modification of NaX Zeolites: The Cobalt (II)-Exchange Kinetics and Surface Property Changes under Thermal Treatment," *Journal of Chemistry*, vol. 2016, Mar. 2016, Art. no. e1789680, https://doi.org/10.1155/2016/1789680.

[29] O. Levenspiel, *Chemical Reaction Engineering*. New York, NY, USA: John Wiley & Sons, 1998.